Depolarization of decaying counterflow turbulence in He II

C. F. Barenghi,[1] A. V. Gordeev,[2] and L. Skrbek[2,3]
[1]*School of Mathematics, University of Newcastle, Newcastle upon Tyne, NE1 7RU, United Kingdom*
[2]*Institute of Physics ASCR, Na Slovance 2, 182 21 Prague, Czech Republic*
[3]*Faculty of Mathematics and Physics, Charles University, V Holešovičkách 2, 180 00 Prague, Czech Republic*
(Received 9 May 2006; published 30 August 2006)

We present experimental evidence backed up by numerical simulations that the steady-state vortex tangle created in He II by heat-transfer counterflow is strongly polarized. When the heater that generates the counterflow turbulence is switched off, the vortex tangle decays, the vortex lines randomize their spatial orientation and the tangle's polarization decreases. The process of depolarization slows down the recovery of the transverse second sound signal which measures the vortex line density; at some values of parameters it even leads to a net *decrease* of the amplitude of the transverse second sound prior to reaching the universal $-3/2$ power temporal law decay typical of classical homogeneous isotropic turbulence in a finite-sized channel.

DOI: 10.1103/PhysRevE.74.026309 PACS number(s): 47.27.−i, 67.40.Vs, 47.37.+q

I. INTRODUCTION

Quantum turbulence [1,2] has been investigated since the pioneering thermal counterflow experiments of Vinen [3] half a century ago, but the underlying physics is far from being fully understood. This is perhaps not surprising. The most recent studies have revealed that quantum turbulence is similar to turbulence in ordinary fluids [2], often regarded as the last unsolved problem of classical physics. The connection between quantum turbulence and classical turbulence is indisputable in experiments in which quantum turbulence is generated in liquid helium using classical techniques, notably by towing a grid through a stationary sample [4–6], or by oscillating the grid (both in He II [7] and ^{3}He-B [8]), or by stirring liquid helium with counter-rotating cylinders [9].

On the contrary, thermal counterflow is a form of motion peculiar to superfluid hydrodynamics [10] and has no analog in an ordinary viscous fluid. For this reason it was often stated that counterflow turbulence in He II has nothing to do with classical turbulence, but recent experiments seem to suggest otherwise [11]. It is known [10] that He II behaves like the intimate mixture of two copenetrating fluid components: the viscous normal fluid (of density ρ_n and velocity $\mathbf{v}_n$) and the inviscid superfluid (of density ρ_s and velocity $\mathbf{v}_s$), where $\rho=\rho_n+\rho_s$ is the total density of liquid helium. Thermal counterflow is set up by applying a voltage to a resistor (heater) located at the closed end of a channel open to the helium bath at the other end. The heat flux is carried away from the heater by the normal fluid alone, and, by conservation of mass, a superfluid current arises in the opposite direction. In this way a relative velocity (counterflow) $v_{ns}=|\mathbf{v}_n-\mathbf{v}_s|$ is created along the channel which is proportional to the applied heat power. At relatively small values of v_{ns} the heat-flow transfer becomes turbulent due to the appearance of an apparently disordered tangle of superfluid vortex lines. The intensity of the turbulence is represented by the vortex line density L (total length of vortex lines, Λ, divided by the volume b^3), which is measured by detecting the extra attenuation of a second sound resonance wave excited between transducers across the channel. Clearly, if one attempted to find a possible connection between counterflow turbulence and classical turbulence, the likely candidate would be turbulent thermal convection. In fact, as noticed in Ref. [11], the efficiency of the turbulent heat transport in both cases is strikingly similar, in that it depends on the driving temperature difference with a power close to 1/3 [12]. Most investigations of counterflow turbulence were concerned with steady-state heat transfer. In this case the vortex line density which is measured agrees with the steady-state solution of Vinen's phenomenological equation which expresses the dynamical balance between generation and decay terms in the presence of a steady counterflow velocity v_{ns}. Analysis of the problem in terms of vortex dynamics and numerical simulations [13] confirmed Vinen's equation and its predictions in the steady-state regime. It is fair to conclude that steady-state counterflow turbulence is understood relatively well, although there are still some open questions concerning the existence of weak and strong turbulence regimes [1], the possibility that the normal fluid becomes turbulent [14] and an overall description in terms of a single phase diagram [15,16].

The temporal decay of counterflow turbulence, on the contrary, is relatively less understood than the steady-state regime. For example, it has been noted [2,17] since the early experiments [3] that the decay of the vortex line density is slower than predicted by Vinen's equation. Recently, a remarkable connection between the decay of quantum and that of classical turbulence has been established [11]. Measurements performed in two channels of square cross section 6×6 mm^2 and 10×10 mm^2 have shown that during the *late* stage of the decay the vortex line density obeys the law

$$L(t)=\frac{D(3C)^{3/2}}{2\pi\kappa\sqrt{\nu_{\mathrm{eff}}}}(t+t_{vo})^{-3/2}, \tag{1}$$

where t is time, $C=1.62\pm0.17$ [18] is the Kolmogorov constant, $\kappa\approx 10^{-3}$ cm^2/s is the quantum of circulation, D is the channel size [19], t_{vo} is a fitting parameter which represents the virtual origin of the time axis and ν_{eff} is a (temperature dependent) effective kinematic viscosity of order of κ. If, in analogy with the seminal problem of He II in a rotating container, one assumes that the average superfluid vorticity is

κL, it can be shown that the decay law (1) can be derived from a purely classical spectral model of turbulence decay [20].

The aim of this paper is to understand an apparently puzzling feature at the early stage of the observed decay, that the attenuation of the second sound signal across the channel initially *increases* rather than decreases. At first sight, assuming that the tangle is homogeneous and isotropic, an increase of the attenuation would mean that the turbulence becomes stronger, which cannot be (the heater is switched off).

II. EXPERIMENTAL SETUP AND DATA

Our experimental setup has been described in detail in Ref. [21]. The data used in this paper were taken in the channel of square 10×10 mm^2 cross section, which is nominally 11.5 cm long. The second sound sensors were placed at opposite walls across the channel, in the middle of its length. The channel was also equipped with two thermometers placed in its ends, capable of measuring the temperature difference between the closed and open ends in steady-state counterflow turbulence. We have attempted to measure the temperature decay when the heater was switched off and found that it is very fast, beyond the time resolution of our resistance bridge of order of few tenths of a second.

The time evolution of the second sound signal when the heater at the closed end of the channel was switched off is complex and may depend on the channel's geometry [22]. The very early stage of the decay, when the turbulence cannot be treated as isothermal but rather as thermally driven, needs special attention and will be discussed elsewhere. On the other hand, the late stage of the decay obeys the classical Eq. (1) as discussed in our earlier papers [11,21]. Here we are interested in the early to middle stages of the decay, which are characterized by a considerably slower decay rate. What is puzzling is that at some parameters we observed a net *decrease* of the second sound amplitude, as shown in Fig. 1. The vortex line density $L(t)$ is usually determined from the measured second sound amplitude $a(t)$ using the relation [3,4]

$$L(t) = \frac{16\Delta_0}{B\kappa}\left(\frac{a_0}{a(t)} - 1\right), \tag{2}$$

where a_0 is the unperturbed second amplitude with no applied heat into the channel, Δ_0 is the full width at half-height of the second sound resonance peak (typically 10 Hz) and B is the temperature-dependent dissipational mutual friction coefficient [23]. However, Eq. (2) is valid only in the assumption that the vortex tangle is homogeneous and isotropic. It has been shown a long ago in rotating containers [3] that the second sound is not attenuated by quantized vortices if it propagates in the direction along the vortex core. Therefore, if the vortex tangle is polarized and the degree of polarization is not known, the second sound amplitude alone does not provide enough information to calculate the total vortex line density. This is why we plot in Fig. 2 the quantity $a_0/a(t)-1$, not the total vortex line density, which we do not know. In our previous paper [21] we speculated that the increase in time of the quantity $a_0/a(t)-1$ can be explained by the fact that the vortex tangle in the steady-state counterflow turbulence is highly polarized by the applied counterflow; therefore, when the heater is switched off, the orientation of the vortex lines becomes more random. To confirm this interpretation we have performed the numerical simulations described in the next section.

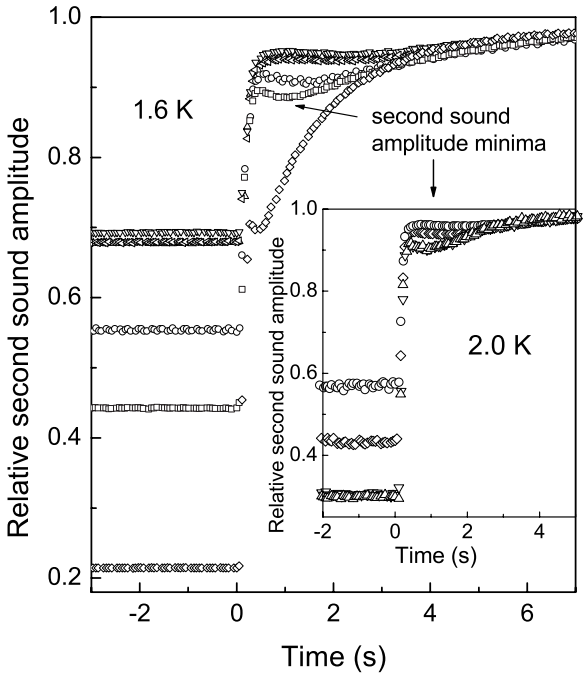

FIG. 1. Relative amplitude $a(t)/a_0$ of the transverse second sound standing mode $a(t)$ at $T=1.6$ K versus time, where a_0 is the unperturbed amplitude with no applied heat into the channel. Negative time corresponds to the initial steady-state counterflow turbulence generated by applying powers: 0.5 W (◇), 0.23 W (□), 0.18 W (○), and 0.14 W (various triangles) to the resistor before located at the closed end. Three different decay curves are shown to illustrate the level of reproducibility for the lowest applied power. At $t=0$ the power is switched off and the second sound amplitude gradually recovers to its unperturbed value. The inset shows analogical data measured at $T=2.0$ K; applied powers: 0.52 W (various triangles), 0.41 W (◇), and 0.32 W (○). Note that the recovery process is not monotonic; at most applied powers the amplitude has another local minimum, marked by arrows.

III. NUMERICAL SIMULATIONS

Following Schwarz [13], we represent superfluid vortex lines as space curves $\mathbf{s}(t,\xi)$ which move according to [24]

$$\frac{d\mathbf{s}}{dt} = \mathbf{v}_s + \mathbf{v}_i + \alpha\mathbf{s}' \times (\mathbf{v}_n - \mathbf{v}_s - \mathbf{v}_i), \tag{3}$$

where the prime denotes differentiation with respect to arclength ξ, $\alpha = B\rho_n/(2\rho)$ is a friction coefficient and $\mathbf{v}_i$ is the self-induced velocity of the vortex line. At a given point $\mathbf{s}$, the self-induced velocity $\mathbf{v}_i$ is given by the Bio-Savart law

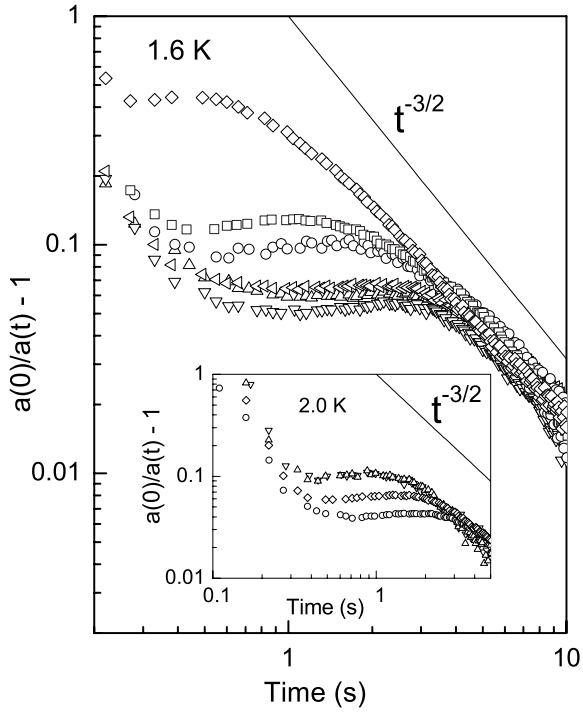

FIG. 2. Log-log plot of the quantity $[a_0/a(t)-1]$ versus time measured at $T=1.6$ K. Under the assumption that the tangle is homogeneous and isotropic, this quantity would be proportional to the vortex line density L. For given experimental conditions, the level $a(t)/a_0-1=0.1$ would correspond to the vortex line density $L\approx 10^5$ cm^{-2}. For details, see text. The different decay curves correspond to different initial levels of steady-state counterflow turbulence generated at powers 0.5 W (◇), 0.23 W (□), 0.18 W (○), and 0.14 W (various triangles), respectively. Three individual decay curves are shown to appreciate the level of reproducibility for the lowest applied power. The inset shows analogical data measured at $T=2.0$ K; applied powers: 0.52 W (various triangles), 0.41 W (◇), and 0.32 W (○).

$$\mathbf{v}_i(\mathbf{s},t)=\frac{\kappa}{4\pi}\oint\frac{(\mathbf{r}-\mathbf{s})\times d\mathbf{r}}{|\mathbf{r}-\mathbf{s}|^3}, \tag{4}$$

where the line integral extends over the entire vortex configuration. The numerical technique to discretize the vortex filaments, to integrate Eq. (3) and to desingularize the Biot-Savart integral (4) are standard (see Refs. [13,27] and references therein). All calculations are performed in a periodic box of size $b=1$ cm. It is common in the literature to use the following local induction approximation (LIA) to the exact Biot-Savart law:

$$\mathbf{v}_i\approx\beta\mathbf{s}'\times\mathbf{s}'', \tag{5}$$

where $\beta=\kappa/(4\pi)\ln[1/(s''a_0)]$ and $a_0\approx 10^{-8}$ cm is the vortex core radius. The use of LIA is computationally convenient, because the cpu time is proportional to the number of discretization points, N, along the vortex filaments, whereas the cost of the Biot-Savart law grows with N^2. In general, given a particular problem, it is not altogether clear if the LIA is sufficiently accurate. Experience shows that in some problems the LIA is a good approximation [13], but in others (rotating turbulence [25]) the Biot-Savart law is necessary. There are also cases (vortex knots [26]) in which the LIA fails.

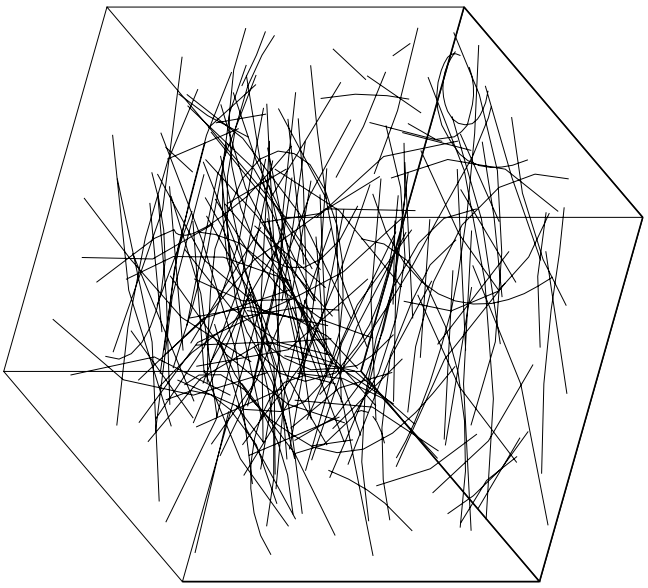

FIG. 3. Computed vortex tangle at the end of the growth stage.

The results presented in this paper are obtained using the Biot-Savart law, but we have also done some runs using the LIA for the sake of comparison.

First, a vortex tangle is produced by applying a uniform counterflow: $\mathbf{v}_n=(0,0,1)$ cm/s, $\mathbf{v}_s=(0,0,0)$, for simplicity along the z direction upon an initial arbitrary vortex configuration (three vortex rings set at random positions and orientation). Because of the friction (we use $\alpha=0.3$ that approximately corresponds to the experimental data measured at 2 K shown in the insets of Figs. 1 and 2), energy is quickly fed into the superfluid vortices, which grow in size [27], reconnect with each other and form a disordered tangle, as shown in Fig. 3. We stop the growth when the total vortex length is $\Lambda=188.9$ cm (a larger vortex length would not be practical due to the computational cost of the Biot-Savart law). As noted first by Schwarz [13] and then confirmed in the experiments [28], the counterflow tangle thus generated is not isotropic. In our case the Cartesian projections of the vortex length along the x, y, and z directions are, respectively, $\Lambda_x=119.4$ cm, $\Lambda_y=120.7$ cm, and $\Lambda_z=6.81$ cm, hence the polarization is expressed by the three ratios $\Lambda_x/\Lambda=0.63\approx\Lambda_y/\Lambda=0.64$ which is much larger than $\Lambda_z/\Lambda=0.04$. These values mean that the vortex loops are flattened in the xy plane perpendicular to the counterflow direction z. This pancakelike structure is revealed in Figs. 4(a) and 4(b) which show transverse and longitudinal views of the vortex configuration.

Second, we reset $t=0$, $\mathbf{v}_n=0$, and allow the tangle to decay under the action of the Biot-Savart law and the same friction $\alpha=0.3$. The time behavior of the projected lengths Λ_x, Λ_y, and Λ_z are shown in Fig. 5; for the sake of graphical clarity the projected lengths are normalized by the values at the beginning of the decay, $\Lambda_x(0)=119.4$ cm, $\Lambda_y(0)=120.7$ cm, and $\Lambda_z(0)=6.18$ cm. It is apparent that,

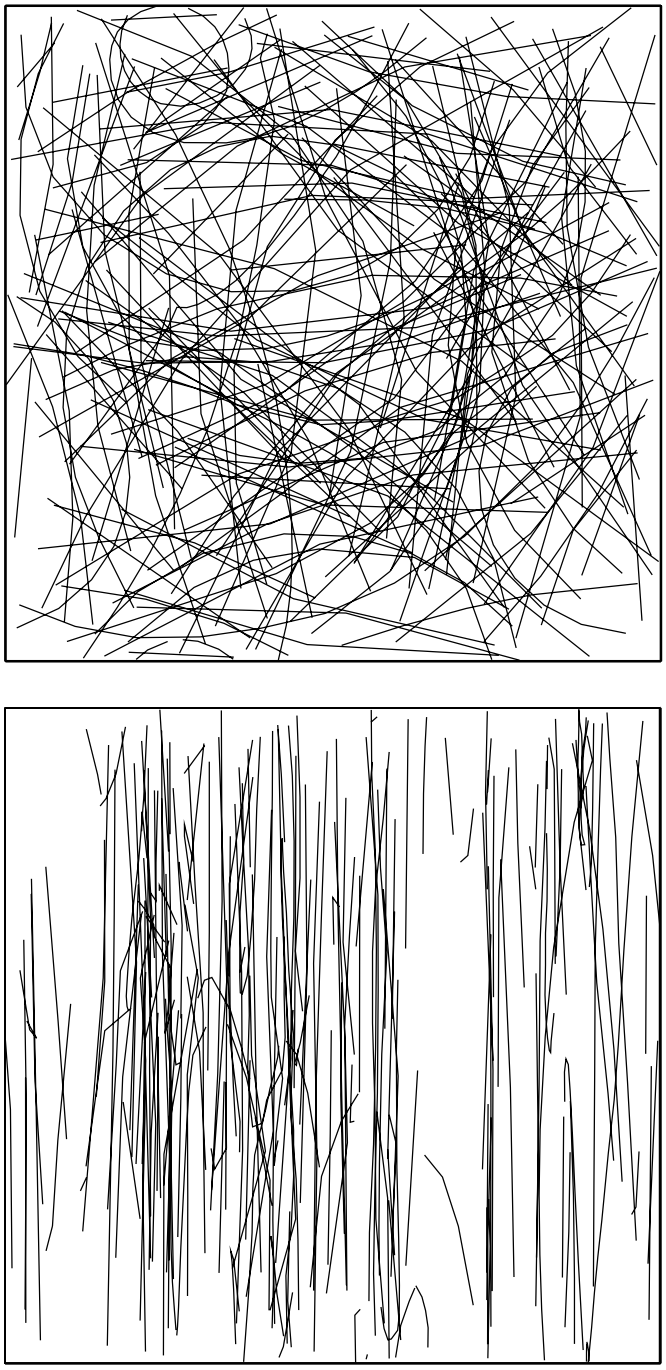

FIG. 4. Projections onto the xy plane (top) and the xz plane (bottom) of the vortex tangle of Fig. 3.

whereas Λ_x and Λ_y decrease with time, Λ_z at first increases, in qualitative agreement with the experimental observations. Transverse and longitudinal views of the vortex tangle at $t=0.1$ s when $\Lambda=121.6$ cm are shown in Fig. 6; clearly the increase of Λ_z is due to vortex loops which randomize their spatial orientation when the normal flow is switched off. Essentially, the vortex tangle depolarizes with time. At this time $t=0.1$ s the decaying tangle is still anisotropic ($\Lambda_x=71.9$ cm, $\Lambda_y=69.7$ cm, and $\Lambda_z=33.6$ cm) but the polarization ratios are now $\Lambda_x/\Lambda=0.59\approx\Lambda_y/\Lambda=0.57$ which is of the same order of magnitude as $\Lambda_z/\Lambda=0.28$. Indeed, Fig.

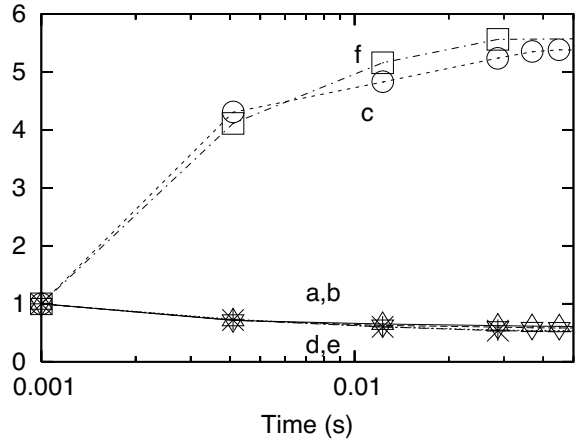

FIG. 5. Relative projected lengths $\Lambda_x(t)/\Lambda_x(0)$ (a, triangles pointing up), $\Lambda_y(t)/\Lambda_y(0)$ (b, triangles pointig down), and $\Lambda_z(t)/\Lambda_z(0)$ (c, squares) versus time during the decay; the values at the beginning of the decay are $\Lambda_x(0)=119.4$ cm, $\Lambda_y(0)=120.7$ cm, and $\Lambda_z(0)=6.81$ cm. Also plotted are the same quantities $\Lambda_x(t)/\Lambda_x(0)$ (d, crosses), $\Lambda_y(t)/\Lambda_y(0)$ (e, diagonal crosses) and $\Lambda_z(t)/\Lambda_z(0)$ (f, circles) but computed using the LIA starting from the same initial state.

7(b) shows that the pancakelike stucture is still visibly but much less marked than in Fig. 4(b).

A natural question to ask is whether the depolarization effect is present if, starting from the same initial condition at the beginning of the decay, the time evolution of the vortex lines is computed using the local induction approximation instead of the exact Biot-Savart law. The additional points marked on Fig. 5 show that the LIA gives a fairly good approximation to the correct evolution. This result is perhaps a bit surprising due to the anisotropy of the initial configuration, but suggests that the depolarization of the tangle when $\mathbf{v}_n$ is suddenly set to zero is an effect driven more by vortex reconnections than by long-range velocity fields. This

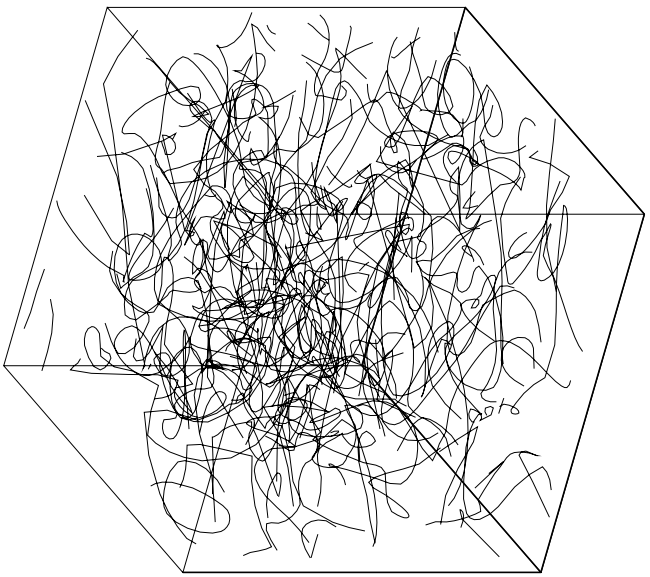

FIG. 6. Computed vortex tangle at $t=0.1$ s during the decay stage.

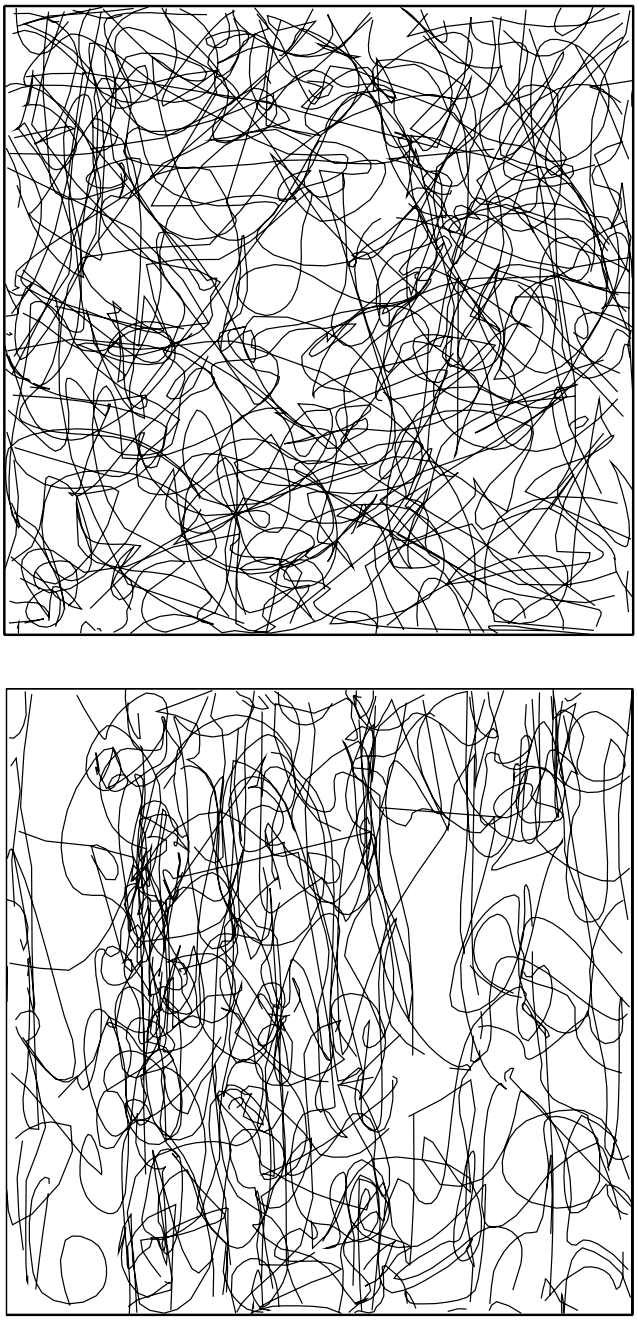

FIG. 7. Projections onto the xy plane (top) and the xz plane (bottom) of the vortex tangle of Fig. 6.

conclusion must be taken with caution, however, because there is no reason to think that the LIA is still a good approximation to the Biot-Savart law if the vortex line density is much larger and the vortex lines are closely packed together.

In summary, the numerical result confirms in a qualitative way our earlier conjecture [21] that, once the heater is switched off, the vortices randomize.

IV. DISCUSSION

What is detected by the second sound sensors in the experiment, however, is not the total vortex length, nor the individual projected lengths. It can be shown [29] that the attenuation of a second sound wave of angular frequency ω in the presence of a straight vortex line is $\sin^2(\gamma)\Omega B/(2\omega)$, where γ is the angle between the vortex line and the direction of sound propagation, $\mathbf{\Omega}$ is the vorticity and $\Omega=|\mathbf{\Omega}|$. This sine squared law has been confirmed experimentally by measuring second sound signals in a container of helium held at tilted angles with respect to the axis of rotation of the cryostat [30]. A consequence of this law is that there are in principle two limiting cases. If the tangle is fully polarized and all vortices are on planes perpendicular to the direction of the counterflow, since $\langle\sin^2(\gamma)\rangle=1/2$ averaged over the unit disk, the sensors detect $L/2$. If the tangle is isotropic, since $\langle\sin^2(\gamma)\rangle=2/3$ averaged over the unit sphere, the second sound sensors detect $2L/3$, where L is the actual vortex line density, a factor of $4/3$ higher [31].

To make better contact between the experiment and the numerical simulation we proceed in the following way. Our computed vortex tangle is discretized into a large number of points (about 4000 during the decay stage). Consider the straight vortex segment $\mathbf{\Omega}=\kappa\mathbf{\Lambda}=\kappa(\Lambda_x,\Lambda_y,\Lambda_z)$ joining two points, where $\Lambda_x=\Lambda\cos(\gamma_1)$, $\Lambda_y=\Lambda\cos(\gamma_2)$, $\Lambda_z=\Lambda\cos(\gamma_3)$, $\Lambda=|\mathbf{\Lambda}|=\sqrt{\Lambda_x^2+\Lambda_y^2+\Lambda_z^2}$, and γ_i $(i=1,2,3)$ are the directional cosines with $\gamma_1^2+\gamma_1^2+\gamma_3^2=1$. Each segment contributes an amount proportional to $\Delta S_x=\Lambda\sin^2(\gamma_1)=(\Lambda_y^2+\Lambda_z^2)/\Lambda$ to the attenuation of a second sound wave propagating in the x direction. Similarly, the contributions to the attenuation of second sound traveling in the y and z directions are $\Delta S_y=(\Lambda_x^2+\Lambda_z^2)/\Lambda$ and $\Delta S_z=(\Lambda_x^2+\Lambda_y^2)/\Lambda$, respectively. By summing ΔS_x, ΔS_y, and ΔS_z over the entire collections of segments, we obtain the quantities S_x, S_y, and S_z, which are proportional to the second sound attenuation along x, y, and z. The time dependence of S_x, S_y, and S_z during the decay (which we plot in a normalized way for better comparison), is shown in Fig. 8. It is apparent that the transverse attenuations (S_x and S_y) decay slower than the longitudinal attenuation, S_z. This is in qualitative agreement with our interpretation of the experimental data (some of the attenuation curves measured at 1.6 K and 2 K shown in Fig. 1 reach a pleateau, or even increase, before decaying). The slower rate of decay of the transverse attenuation, or the fact that it reaches a pleateau or even increases, is something which is likely to depend on the vortex line density, amount of polarization and friction α. Due to the arbitrariness of the initial state in our decay model, quantitative predictions are not possible. Some qualitative insight about behavior on a slightly longer time scale than in Fig. 5 can perhaps be inferred using the computational convenient LIA. As said before, we have no reason to think that the LIA is still a good approximation to the Biot-Savart law for larger Λ, but we do the following numerical experiment: starting from few seeding vortex loops as before, first we impose $\mathbf{v}_n=(0,0,1)$ cm/s and create a vortex tangle at $\alpha=0.1$ (this approximately corresponds to the data measured at 1.6 K) with the LIA; the properties of this tangle are $\Lambda=363.5$ cm, $\Lambda_x=231.4$ cm, $\Lambda_y=231.1$ cm, $\Lambda_z=16.34$ cm, $S_x=182.5$, $S_y=183.0$, and $S_z=361.4$. Second we set $\mathbf{v}_n=0$ and let the tangle decay under LIA and the same $\alpha=0.1$. The resulting attenuation curves are shown in Fig. 9: again, note that whereas S_z decreases, S_x and S_y have pro-

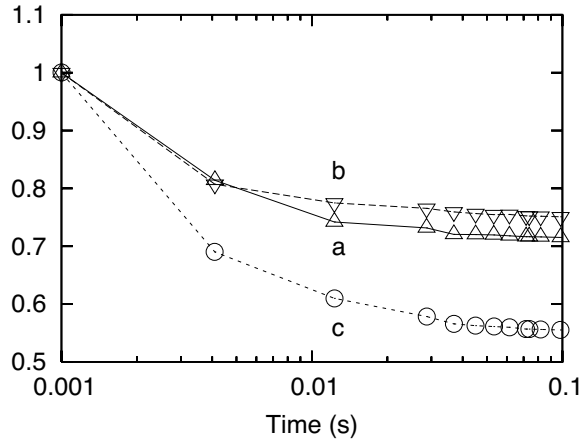

FIG. 8. Plot of S_x/S_x^0 (a, triangles pointing up), S_y/S_y^0 (b, triangles pointing downs), and S_z/S_z^0 (c, circles) versus time; the quantities S_x, S_y, and S_z, defined in the text, are proportional to the observed second sound signal propagating in the x, y, and z directions, respectively, according to the sine square law. The normalizing values $S_x^0=95.4$, $S_y^0=93.9$, and $S_z^0=188.4$ are the values of S_x, S_y, and S_z at the start of the decay. Note the relatively slower decay of the transverse signals S_x and S_y.

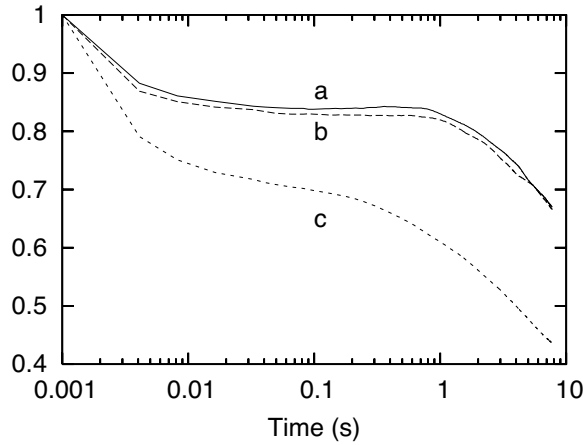

FIG. 9. Plot of S_x/S_x^0 (a), S_y/S_y^0 (b), and S_z/S_z^0 (c) versus time over a longer time range according to the LIA with $\alpha=0.1$. The normalizing values $S_x^0=182.5$, $S_y^0=183.0$, and $S_z^0=361.4.4$.

longed plateaus before they eventually decrease at larger time, again in qualitative agreement with the experiment.

V. CONCLUSIONS

Before concluding, some words of caution are necessary. The experimentally observed temporal decay of the counterflow He II turbulence is very complex, displays several regimes and the details depend on various factors as the channel geometry, starting level of the counterflow steady-state turbulence and temperature. The described secondary minimum in the second sound amplitude was not observed over the entire parameter space covered by the experiments, but is clearly visible during the early decay phase over a robust range of heat flux as shown in Fig. 1. Clearly the effect is at first puzzling: why should the second sound attenuation level out or even increase rather than decrease when the heater is switched off? Similarly, it must be kept in mind that the numerical simulations are necessarily idealized. The numerical model refers to vortex line densities much lower than in the experiments and does not include the effects of the channel's boundaries on the decay of the vortex tangle. Perhaps more important is the fact that the initial state of the computed decay is arbitrary; it is obtained by interrupting a driven growth stage, so it does not correspond to a statistical steady-state counterflow turbulence at a certain value of α.

The simulation also assumes that the normal fluid is perfectly stationary, although in reality the normal fluid (either laminar or turbulent [14]), must have its own decay time scale. Our simulation necessarily ignores any flow that might be induced by the vortex tangle in the normal fluid. A proper account of this possible effect would need solving coupled equations describing motion of both fluids, which at present is beyond our scope. Let us mention here that an attempt to couple the normal fluid was made by Schwarz and Rosen [17], who simulated turbulence in the normal fluid by an eddy of a fixed size. That the late decay displays the classical power law suggests normal fluid turbulence might be an issue.

Still, the numerical evidence is robust: the counterflow vortex tangle is polarized, and, once the normal fluid is set to zero, the vortex lines depolarize and the projected vortex length in the direction along the channel axis, Λ_z, increases before decaying later. Because of this depolarization, the transverse second sound signal does not decay immediately. The qualitative agreement between the experiments and the numerical simulations confirms earlier evidence that counterflow turbulence is strongly polarized [28] and solves the apparent experimental puzzle that, when the heater which generates the turbulence is switched off, the transverse second sound attenuation appears to increase rather than decrease.

ACKNOWLEDGMENTS

The authors acknowledge stimulating discussions with a number of colleagues, especially with T. V. Chagovets, M. Tsubota, and W. F. Vinen. This research is supported by the Institutional Research Plan AVOZ10100520, by the Czech Grant Agency under Grant No. GAČR 202/05/0218, and by EPSRC (Grants Nos. GR/T08876/01 and EP/D040892/1).

[1] J. T. Tough, "Superfluid turbulence," *Progress in Low Temperature Physics* (North-Holland, Amsterdam, 1982), Vol. VIII.
[2] W. F. Vinen and J. J. Niemela, J. Low Temp. Phys. **128**, 167 (2002).
[3] H. E. Hall and W. F. Vinen, Proc. R. Soc. London, Ser. A **238**, 204 (1956); W. F. Vinen, *ibid.* **240**, 114 (1957); **242**, 489 (1957).
[4] M. R. Smith, R. J. Donnelly, N. Goldenfeld, and W. F. Vinen, Phys. Rev. Lett. **71**, 2583 (1993).
[5] S. R. Stalp, L. Skrbek, and R. J. Donnelly, Phys. Rev. Lett. **82**, 4831 (1999).
[6] L. Skrbek, J. J. Niemela, and R. J. Donnelly, Phys. Rev. Lett. **85**, 2973 (2000).
[7] S. I. Davis, P. C. Hendry, and P. V. E. McClintock, Physica B **280**, 43 (2000).
[8] D. I Bradley, D. O. Clubb, S. N. Fisher, A. M. Guenault, R. P. Haley, C. J. Matthews, G. R. Pickett, V. Tsepelin, and K. Zaki, Phys. Rev. Lett. **96**, 035301 (2006).
[9] J. Maurer and P. Tabeling, Europhys. Lett. **43**, 29 (1998).
[10] L. D. Landau and E. M. Lifshitz, *Fluid Mechanics* (Pergamon, New York, 1987).
[11] L. Skrbek, A. V. Gordeev, and F. Soukup, Phys. Rev. E **67**, 047302 (2003).
[12] C. E. Chase, Phys. Rev. **127**, 361 (1962); **131**, 1898 (1963).
[13] K. W. Schwarz, Phys. Rev. B **38**, 2398 (1988).
[14] D. J. Melotte and C. F. Barenghi, Phys. Rev. Lett. **80**, 4181 (1998).
[15] G. E. Volovik, JETP Lett. **78**, 553 (2003).
[16] L. Skrbek, JETP Lett. **80**, 474 (2004).
[17] K. W. Schwarz and J. R. Rozen, Phys. Rev. Lett. **66**, 1898 (1991); Phys. Rev. B **44**, 7563 (1991).
[18] K. R. Sreenivasan, Phys. Fluids **7**, 2778 (1995).
[19] Similar behavior was observed in rectangular counterflow channel 1×1 cm^2 (see Fig. 2 of Ref. [4]), but was neither discussed nor systematically investigated. Note also that the scaling with respect to the channel size D, to the best of our knowledge, still remains to be done for classical decaying turbulent flows.
[20] L. Skrbek and S. R. Stalp, Phys. Fluids **12**, 1997 (2000).
[21] A. V. Gordeev, T. V. Chagovets, F. Soukup, and L. Skrbek, J. Low Temp. Phys. **138**, 549 (2005).
[22] An important issue is the time response of the measuring system with regard to the finite velocity of second sound. Calculations show that in most cases (except close to the lambda temperature) there is negligible error introduced into the deduced vortex line density, for the following reasons. For high L, the quality factor of the resonator is very low, of order unity, and the detecting system can be described rather as a second sound pulse technique with the characteristic time response given by the time of flight $d/u_2\sim10^{-3}$ s, where $u_2\sim20$ m/s [23]. As the turbulence decays, the characteristic time constant increases with the (temperature dependent) quality factor. Without the vortex tangle, the typical linewidth of the second sound resonance is 20–100 Hz, the typical frequency used is 2 kHz, so the quality factor reaches 20–100 and the time response gradually rises to about 0.1–1 s at the very end of the decay, where it constitutes an error of less than 1%. There are also other time restrictions than the finite velocity of second sound, such as the time constant of the lock-in amplifier used for detection of the amplitude of the second sound signal.
[23] R. J. Donnelly and C. F. Barenghi, J. Phys. Chem. Ref. Data **27**, 1217 (1998).
[24] In writing Eq. (3) we neglect a term proportional to the smaller mutual friction coefficient B'.
[25] M. Tsubota, T. Araki, and C. F. Barenghi, Phys. Rev. Lett. **90**, 205301 (2003).
[26] R. L. Ricca, D. C. Samuels, and C. F. Barenghi, J. Fluid Mech. **391**, 29 (1999).
[27] C. F. Barenghi, G. G. Bauer, D. C. Samuels, and R. J Donnelly, Phys. Fluids **9**, 2631 (1997).
[28] C. F. Barenghi, C. E. Swanson and R. J. Donnelly, in *75th Jubilee Conference on Helium-4*, edited by J. G. M. Armitage (World Scientific, Singapore, 1983), p. 52; R. T. Wang, C. E. Swanson, and R. J. Donnelly, Phys. Rev. B **36**, 5240 (1987).
[29] The second sound wave equation is $\ddot{\mathbf{q}}+(2-B')\boldsymbol{\Omega}\times\dot{\mathbf{q}}-B\hat{\boldsymbol{\Omega}}\times(\boldsymbol{\Omega}\times\dot{\mathbf{q}})=c^2\boldsymbol{\nabla}(\boldsymbol{\nabla}\cdot\mathbf{q})$ where $\mathbf{q}=\mathbf{v}_n-\mathbf{v}_s$ and c is the second sound speed. Assume that the sound propagates in the x direction, $\mathbf{q}=e^{i\omega t-ikx}(q_x,q_y,0)$, where k is the wave number. Let the vorticity be $\boldsymbol{\Omega}=(\Omega\sin(\theta),0,\Omega\cos(\theta))$ where θ is the angle from the z direction. It is easy to show that, in the typical experimental condition that $\Omega/\omega\ll1$, the wave number is $k=(\omega/c)[1-i\Omega B\cos^2(\theta)/(2\omega)]$. The negative imaginary part of k, $\sin^2(\gamma)\Omega B/(2\omega)$, is the attenuation coefficient, where $\gamma=\pi/2+\theta$ is the angle between the direction of the vorticity and that of the second sound.
[30] H. A. Snyder and Z. Putney, Phys. Rev. **150**, 110 (1966); P. Mathieu, B. Placais, and Y. Simon, Phys. Rev. B **29**, 2489 (1984).
[31] The original estimate of this depolarization effect given in Ref. [21] was based only on the projected lengths of the fully polarized and random vortex tangles, without taking into account the sine squared law. It increases the maximum depolarization effect (assuming constant L) that could be detected by the second sound attenuation by about 10%, from $\pi^2/8$ to $4/3$ calculated here.